

# CONSIDERATIONS FOR THE PARAMETERISATION OF A CHATTER DETECTION ALGORITHM

CHRISTIAN BRECHER<sup>1</sup>, PAUL WEILER<sup>1</sup>,  
RALPH KLIMASCHKA<sup>1</sup>, STEPHAN NEUS<sup>1</sup>

<sup>1</sup>Laboratory for Machine Tools and Production Engineering  
WZL of the RWTH Aachen University, Germany  
DOI: 10.17973/MMSJ.2024\_03\_2023145  
r.klimaschka@wzl.rwth-aachen.de

Process instabilities due to the regenerative effect limit the material removal rate of cutting machine tools. A method developed at the Laboratory for Machine Tools and Production Engineering (WZL) at RWTH Aachen University reduces the experimental effort of determining stability limits for milling. The method bears on a time-domain chatter detection algorithm, which detects process instability based on predefined threshold values. Up to now, the definition of the threshold values has been derived from a selective number of sample tests. To investigate the transferability of the chatter detection algorithm to various boundary conditions cutting tests are carried out. In addition, a new stability criterion for high frequency chatter oscillations is introduced. The results are analysed with regard to factors that require an adjustment of the threshold values. Based on the results, a parameterisation of the chatter detection algorithm is presented.

## KEYWORDS

Regenerative chatter, chatter detection, time-domain chatter detection algorithm, Poincaré section, parameterisation

## 1 INTRODUCTION

Machine tools are exposed to high demands regarding productivity, product quality and resource efficiency in a globalised market environment. A main limiting factor for increasing the productivity of cutting machine tools remains to be the occurrence of process instabilities induced by self-excited machine vibrations. [Altintas 2020] The most frequent cause of self-excited machine vibrations is the regenerative effect. Its consequences can be insufficient surface quality, increased tool wear, tool breakage and damage to the machine tool. [Kayhan 2009; Yusoff 2011] In order to optimise the metal removal rate and thus the productivity of a machine tool without exceeding the limits of process stability, the determination of stability lobe diagrams (SLD) is suitable. In a SLD, the stability limit, which is characterised by the parameters critical cutting depth  $a_{p,crit}$  and the critical spindle speed  $n_{crit}$ , is plotted for a given system of machine tool, tool and workpiece. [Quintana 2011] When determining SLD, a distinction is made between experimental and simulative approaches. Simulative approaches are based on modified versions of the chatter control loop developed in [Merritt 1965], whereby the occurrence of the regenerative effect is described analytically. [Altintas 1995] For the parameterisation of the chatter control loop, knowledge of the machine structure direct and cross function as well as the dynamic cutting force coefficients are required, which are obtained through extensive measurements. [Altintas 2004; Altintas 2008] In addition to a

high metrological effort, a complex implementation limits the industrial application of simulative approaches. In the conventional determination of experimental SLD, the cutting depth is increased at a constant spindle speed in discrete steps until process instability occurs. The spindle speed is then increased and the process of discrete depth-of-cut increase is repeated. The number of cutting tests correlates with the desired resolution of the SLD. Experimental SLD represent the real stability limit of a machine tool-workpiece-tool system, whereby their determination is time consuming and expensive. An efficient method for producing experimental SLD is offered by an algorithm presented at the Laboratory for Machine Tools and Production Engineering WZL at the RWTH Aachen University. By combining existing approaches in which the cutting depth [Quintana 2008] or the spindle speed [Grossi 2015; Brecher 2017] is continuously increased, the time required to determine SLD is reduced by up to 90 % compared to conventional methods, while at the same time increasing the resource efficiency. To reliably detect process instability, a sensor-based measurement method is used. [Brecher 2021]

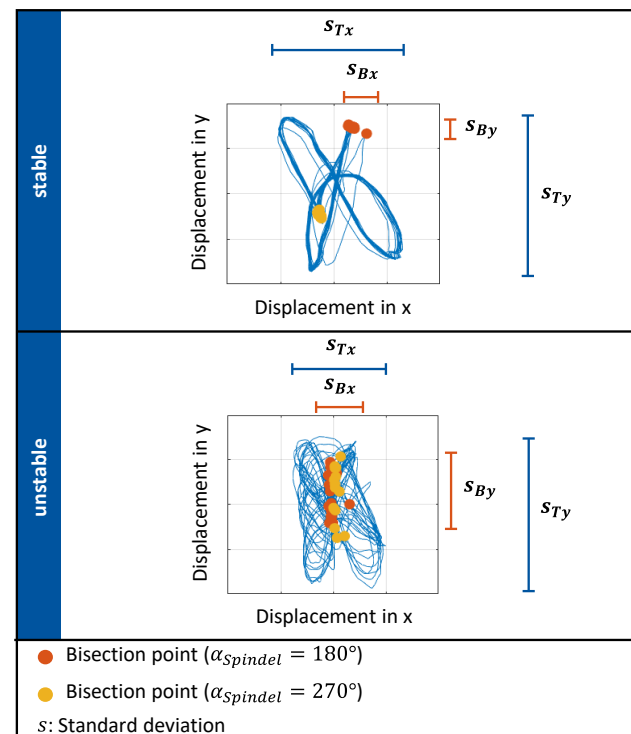


Figure 1 : Trajectory of a stable and an unstable cutting process

## 2 SENSOR BASED CHATTER DETECTION

Sensor-based measurement methods for the detection of process instability can be classified by time-based and frequency-based approaches. [Navarro-Devia 2023] Frequency-based approaches use the characteristic of a sudden increase in the amplitude of self-excited oscillations, when the critical cutting depth  $a_{p,crit}$  is exceeded. In the spectrum, process instability is expressed by high amplitudes close to a natural frequency of the machine tool-workpiece-tool system. The deficits of the frequency-based approaches are, besides a low resolution with short measuring times, the fact that the regenerative effect is only detected after its occurrence and not during its emergence. [Perrelli 2022]

Time-domain based approaches, on the other hand, offer the advantage of detecting process instability online, without prior knowledge of natural frequencies of the machine tool-workpiece-tool system. In [Davies 1998], [Brecher 2015] and

[Honeycutt 2016] time-domain based approaches are presented, which utilise Poincaré maps. In Poincaré maps, the approximated displacement of the tool centre point (TCP) along a spindle revolution in the machining plane is measured by a sensor and displayed as a trajectory in a coordinate system. As shown in Figure 1, a stable cutting process is characterised by a regular trajectory course, whereas process instability is characterised by a chaotic trajectory course. In addition, so-called bisection points are shown in Figure 1. Bisection points describe the displacement of the TCP at a defined angular position of the spindle  $\alpha_{spindle}$ . Based on the bisection points, the bisection indicator ( $BI$ ), given in formula (1), is developed. The bisection indicator is defined by the standard deviation of the bisection points ( $s_{Bx}, s_{By}$ ) related to the standard deviation of the total trajectory ( $s_{Tx}, s_{Ty}$ ). [Brecher 2015]

$$BI = \frac{s_{Bx} \cdot s_{By}}{s_{Tx} \cdot s_{Ty}} \quad (1)$$

For the stability evaluation of a cutting process, stability criteria are developed based on the bisection indicator (see Figure 2), which are implemented in a time-domain chatter detection algorithm. In order to detect the characteristic amplitude jump of a self-excited oscillation, the jump criterion is introduced. The jump criterion compares the current bisection indicator with the mean value of the last five bisection indicators. If the jump criterion exceeds a previously defined jump factor, process instability is indicated. A continuous increase in machine vibration is detected using the trend criterion, which considers the slope between two bisection points. If the trend criterion exceeds a defined trend factor three times in a row, process instability is indicated. In order to compensate for the deficits of the trend criterion in the case of noisy measurement signals, the gradient criterion is introduced, which is calculated by the slope between the current bisection point and the fifth last bisection point. If the slope exceeds a defined gradient factor, process instability is detected. To avoid damage to the machine tool as a result of process instability the limit criterion is introduced as an absolute value of the bisection indicator. [Brecher 2018]

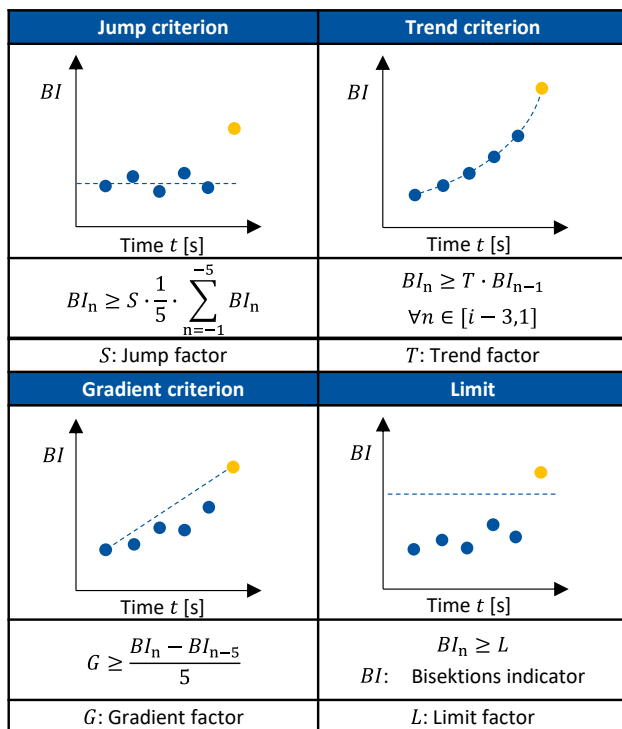


Figure 2 : Stability criteria for the detection of the regenerative effect

Time-domain based stability criteria have the deficit that process instability is not detected by a unique criterion. As can be seen from the presented chatter detection, the stability evaluation is realised by empirically determined threshold values. Ideally, the threshold values of the bisection indicator are set manually once, as the bisection indicator only evaluates the relative change in the trajectories and not the dynamics of the machine tool-workpiece-tool system. In order to evaluate the transferability of the threshold values to varying boundary conditions, the influence of various factors on the threshold values of the chatter detection algorithm is investigated in this paper. The aim of the cutting tests is to obtain an overview of factors that require an adjustment of the threshold values of the chatter detection algorithm and to consolidate the correlations discovered in parameter sets. To increase the robustness of the chatter detection algorithm, an additional indicator is first introduced to evaluate the process stability.

### 3 SMOOTHNESS INDICATOR FOR THE EVALUATION OF PROCESS STABILITY

From the experimental results of [Brecher 2018] and [Brecher 2021] it can be seen that process instability is reliably detected using the bisection indicator for low frequency structural modes. An acceleration sensor is positioned on the spindle housing to record the system vibrations. In the course of further test series, deficits of the existing chatter detection algorithm based on Poincaré maps become apparent for various machine tools when high frequency spindle and tool modes occur. High frequency vibrations manifest themselves at the spindle housing measuring position as a superimposed vibration of the fundamental vibration caused by the process force. Due to typically lower amplitudes of high frequency vibrations, the process force related displacement trajectory remain repeatable, so that process instability is not indicated by the bisection indicator. In order to counteract the deficit of the bisection indicator, a smoothness indicator ( $GI$ ) was developed at the WZL of the RWTH Aachen, which is based on the procedure of a roundness measurement (see Figure 3). First, the centre point of a trajectory is identified. Then a distance profile is created by calculating the euclidean distances between the centre point and the reference points of a trajectory. Based on the euclidean distances, a smoothed distance profile is determined with the help of the moving average value. The application of the moving average corresponds to a low pass filter in the frequency domain, so that high frequency displacements are filtered out of the smoothed distance profile. The smoothness indicator is defined by the standard deviations between the measured and the smoothed distance profile.

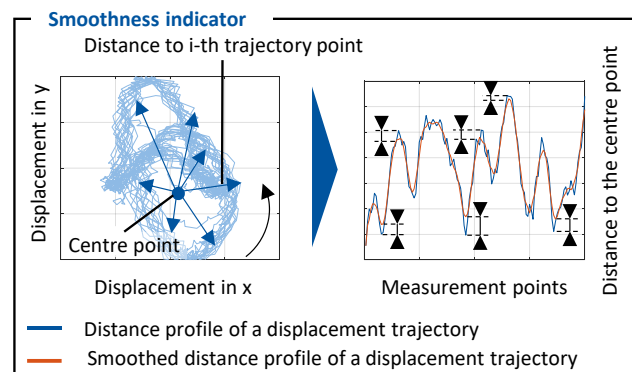


Figure 3 : Concept of the smoothness indicator

The smoothness indicator is defined by the following equation

$$GI = \sqrt{\frac{1}{k-1} \cdot \sum_{i=1}^k (d_{i,m} - \overline{d_{i,m}})^2} \quad (2)$$

where  $k$  describes the number of interpolation points of a trajectory,  $d_{i,m}$  denotes the distance of the  $i$ -th trajectory point to the centre point and  $\overline{d_{i,m}}$  characterises the distance of the  $i$ -th trajectory point to the smoothed trajectory.

Figure 4 shows the result of a spindle speed variation cut on a five-axis vertical machining centre in travelling column design (five axis milling machine) at a cutting depth  $a_p = 1.7$  mm and a spindle speed range of  $3030 \text{ min}^{-1} - 3130 \text{ min}^{-1}$  using the material C45. The tool utilised is a three-toothed milling cutter with a tool diameter of  $d_w = 25$  mm. In the time profile of the acceleration signal as well as in time profile of the bisection and smoothness indicator, an initial amplitude jump can be observed, which characterises the tool run-in behaviour. The tool run-in behaviour describes the phase in which the system is excited impulsively by the initial contact between the tool and the workpiece and then decays. At the time  $t \approx 14$  s, process instability occurs, which is characterised by a sudden increase in the acceleration amplitude as well as a chaotic course of trajectories. From the time profile of the bisection indicator it can be seen that the amplitude jump at the onset of process instability is in the order of magnitude of the signal noise, so that process instability is not indicated through the bisection indicator.

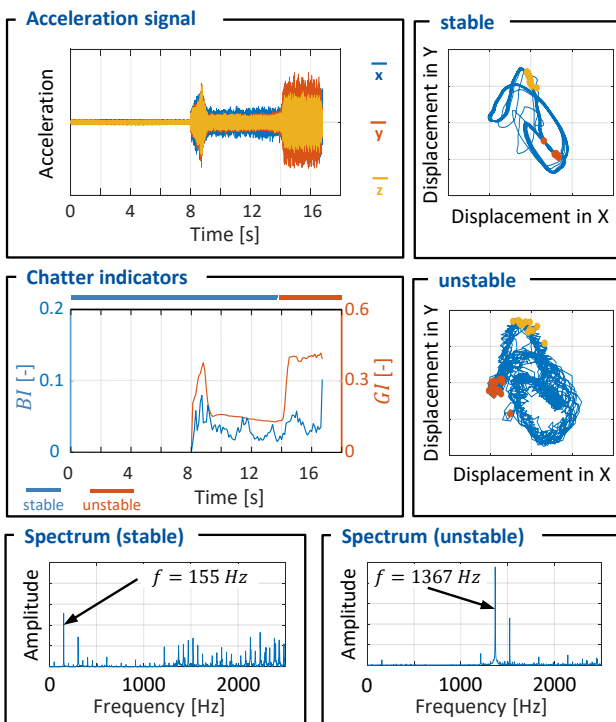


Figure 4 : Process instability induced by a high-frequency mode

The spectrum shown in Figure 4 illustrates that the onset of process instability is accompanied by a shift of the dominant oscillation frequency from 155 Hz (tooth passing frequency) to 1367 Hz. In addition to the sudden increase in acceleration amplitude and a chaotic trajectory, chatter marks on the workpiece surface are also observed as a characteristic feature of process instability due to the regenerative effect. To verify the observations, an experimental modal analysis was performed on the five axis milling machine. The result of the modal analysis yields that there is a pronounced compliance in the Y-direction at a frequency of 1367 Hz, which confirms the regenerative

effect as the cause of the process instability. At the same time, the results of the modal analysis correspond to the dominant acceleration amplitude in the Y-direction during unstable cutting (see Figure 4). The associated mode is a spindle-tool oscillation, as shown schematically in Figure 5. From the sudden increase of the smoothness indicator at the occurrence of process instability (see Figure 4) it is seen that process instability induced by a high frequency mode can be detected by the smoothness indicator. Through additional test series with varying technology parameters and different machine tools, the smoothness indicator was successfully validated and integrated into the existing chatter detection algorithm. The stability criteria of the smoothness indicator are defined analogously to those of the bisection indicator (see Figure 2).

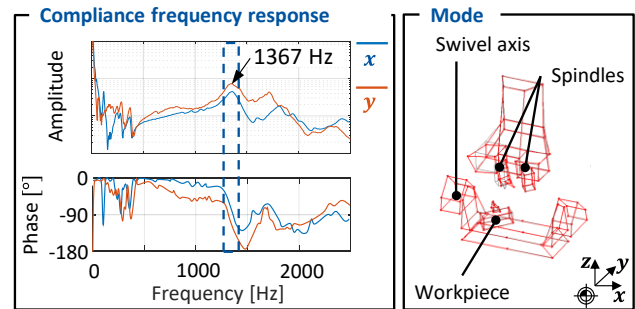


Figure 5 : Result of the experimental modal analysis

The sensitivity of the smoothness indicator in regards to the chosen moving average interval for calculation is shown in Figure 6. The different graphs indicate a different number of points used for the moving average, i.e. the interval length. The corresponding process is known from Figure 4. Firstly, it can be seen that a shorter interval length leads to a lower smoothness indicator. An interval length of 2 points would lead to an identical recreation of the input signal. Consequently, the smaller the interval, the closer the smoothed signal is to the input signal. As the  $GI$  effectively reveals the deviation of the input signal with high frequency parts from the smoothed signal, this trend aligns well with the indicator definition. However, with an increasing interval length the difference between stable and unstable conditions become less apparent since the average is calculated over an increased number of sampled points making it less sensitive to changing conditions. The ideal interval length is mainly dependent on the combination of the acceleration signal sampling rate and the predominant chatter frequency. For the given boundary conditions an empirically determined interval length of 5 yields the best results.

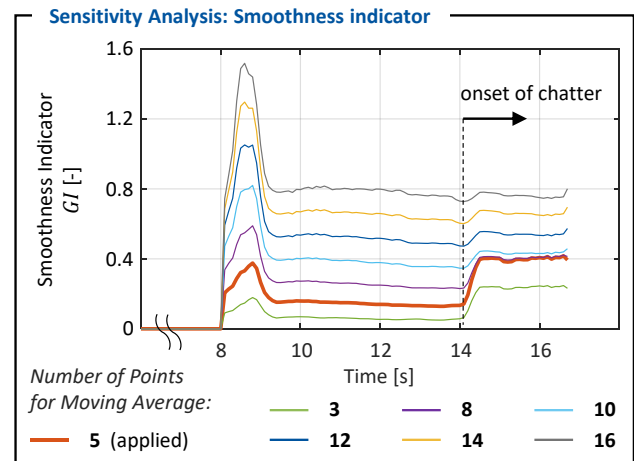


Figure 6 : Influence of the moving average interval on the smoothness indicator

### Factors and their stages

Factor	1. stage ( $S_1$ )	2. stage ( $S_2$ )	PF <sub>1</sub>	PF <sub>2</sub>	FF
Machine tool	4- axis milling machine	5- axis milling machine	x	x	
Workpiece position	**	**	x	x	x
Material	42CrMo4	C45	x	x	x
Tool	milling cutter	end mill	x		x
Feed per tooth	0.1 mm	0.14 mm	x	x	
Slope angle $\alpha_{slope}$	0.4°	0.6°	x	x	
Spindel speed acceleration	$5 \frac{\text{min}^{-1}}{\text{s}}$	$10 \frac{\text{min}^{-1}}{\text{s}}$	x	x	
Engagement width	$d_W$	$0.8 \cdot d_W$			
Rotational direction	synchronous	counter-rotation		x	
Clamping system	vice	5-axis clamping system			x

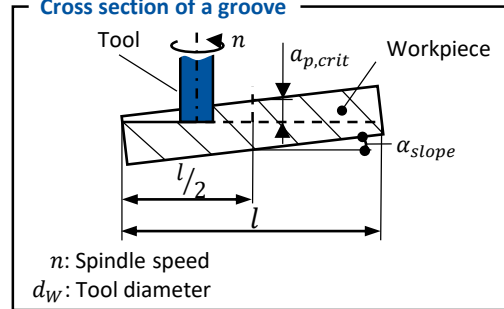
PF<sub>i</sub>: Partial factorial  $2^{7-3}$

experimental design(i)

FF: Full factorial

experimental design

### Cross section of a groove



$n$ : Spindle speed

$d_W$ : Tool diameter

### \*\* Workpiece position

Coordinate	5 axis milling machine	4-axis milling machine
$\Delta x$	92.2 mm	46.2 mm
$\Delta y$	6.1 mm	54.6 mm
$\Delta z$	37.2 mm	0 mm

$\Delta$ : Difference between both measuring positions (workpiece coordinate system)

x: Factors that are varied

Figure 7 : Overview of the structure of the partial factorial (PF<sub>1</sub>, PF<sub>2</sub>) and full factorial experimental (FF) designs

## 4 MEASUREMENT SETUP

In order to systematically investigate varying boundary conditions on the chatter detection algorithm, experimental designs are developed using methods of the design of experiments (DoE). Consideration is given to factors that have an influence on the emergence of the regenerative effect and/or influence the dynamic behaviour of the machine tool-workpiece-tool system. The selection of factors shown in Figure 7 represents a compromise of resources, the application relevance in the determination of SLD and the measurability of the influences on the chatter detection algorithm.

During the cutting tests on a four- axis horizontal milling machine in crossbed design, a four-toothed milling cutter with a tool diameter of  $d_w = 50$  mm is used, which is equipped with indexable inserts of the type R390-18 06 08M-PM 4240. For the five-axis vertical machining centre in travelling column design (5-axis milling machine) a three-toothed milling cutter with a tool diameter of  $d_w = 25$  mm is used, which is equipped with R390-11 T3 08M-PM 4340 inserts. On both machine tools, a four-toothed end mill of type 203007\_16 with a tool diameter of  $d_w = 16$  mm is used. The tools are connected to the spindle via a HSK63 on the four axis milling machine and via a HSK40 on the five axis milling machine.

For an efficient experimental design, partial factorial  $2^{k-p}$  experimental designs are used in addition to full factorial experimental designs, whereby two factor stages ( $S_1$ ,  $S_2$ ) are defined per factor. A full-factorial experimental design offers the advantage of determining all effects and their interactions between selected factors. An interaction indicates how strongly the effect of a factor depends on the factor stage of other factors. The parameter  $k$  describes the number of factors considered in a full-factorial experimental design. With increasing  $k$ , the number of factor stage combinations increases exponentially, where in particular the number of interactions between more than 2 factors, so-called higher-order interactions, increases. Since higher-order interactions are often negligible, it is reasonable to consider additional factors instead of higher-order interactions. This concept is pursued by so-called partial factorial  $2^{k-p}$  experimental designs. The parameter  $p$  describes the number of factors that are analysed instead of

higher-order interactions of a  $2^k$  full factorial experimental design. Partial factorial  $2^{7-3}$  experimental designs are used in the following studies, which means that  $k = 7$  factors are analysed within one experimental design. Compared to a full factorial  $2^4$  experimental design,  $p = 3$  additional factors are considered in place of higher-order interactions. By using a partial factorial  $2^{7-3}$  experimental design, the number of factor stage combinations can be reduced from  $2^7 = 128$  to  $2^4 = 16$  compared to a full factorial experimental  $2^7$  design. [Kleppmann 2020] The reduced experimental effort due to the use of partial factorial  $2^{k-p}$  experimental designs is at the expense of a mixture of effects. In order to ensure that the experimental results are not misinterpreted because of mixing of effects, resolution IV will be selected in the upcoming series of experiments so that the main effects can be reliably determined. Therefore, a partial factorial  $2^{7-3}$  experimental design is used in the experimental series, so that the experimental design contains 16 factor stage combinations. To recognise the effects of the factors on the threshold values of the chatter detection algorithm as clearly as possible, large step sizes are selected between the factor stages. [Siebertz 2017]

The experimental design and the definition of the factor stages (see Figure 7) are made taking into account technical limitations, such as the spindle power, the clamping situation or the recommended cutting speed of a tool.

In order to determine the trajectory of the TCP, a triaxial acceleration sensor from the manufacturer PCB piezotronics with an integrated IEPE (Integrated Electronics Piezo Electric) unit is attached to the spindle housing, analogous to the test series from [Brecher 2018] and [Brecher 2021]. The analogue acceleration signal is converted into a digital signal using the NI-9234 (National Instruments) measuring card, with a sampling rate of  $f_R = 5120$  Hz. In the subsequent signal processing, the acceleration signal is high pass filtered with a cut-off frequency  $f_G = 50$  Hz, trend corrected, periodically regressed and double-integrated to create a sharp trajectory. To generate the bisection points, the angular position of the spindle is taken from the encoder signal of the main spindle motor, pre-processed with the use of an interpolator and recorded by the NI-9411 measuring card. To start or stop a cutting process, a digital input signal is transmitted to the X132 interface of the Numerical Control Unit (NCU) using the NI-9472 measuring card. The input

signal of the X132 interface is evaluated by a synchronous command within the NC programme in the interpolation cycle. All three measuring cards (NI-9234, NI-9411, NI-9472) are integrated in a data acquisition board (DAQ board) of the type NI cDAQ-9174, which is connected to the measuring computer.

A graphical user interface was implemented in the MATLAB development environment and embedded in the evaluation software for efficient experimentation. Technology parameters are transferred via the user interface according to the specifications from the experimental designs, which are then processed by software in the background and transmitted to the NCU in the form of R-parameters. The R-parameters are integrated in a parameterised NC-code, so that different groove configurations can be realised by means of one NC-code. A groove is configured such that a stability transition, characterised by the tuple  $\{a_{p,crit}, n_{crit}\}$ , occurs in the middle of the length  $L$  of a groove ( $0.5 \cdot L$ ). For each factor stage combination, two different stability transitions are considered, whereby two test repetitions are carried out in each case, so that a total of four cutting tests are completed for each factor stage combination. An exception are the cutting tests with the milling cutter on the four axis milling machine, where only one stability transition is taken into account due to the high workpiece consumption as a result of high cutting depths ( $a_p \approx 5.5$  mm). The number of test repetitions represents a compromise between machine load, resource consumption and reproducibility of the test results.

As soon as process instability is perceived acoustically, a digital input signal is sent to the NCU by pressing a button on the user interface, so that the cutting test is stopped. The occurrence of process instability is qualitatively verified on the basis of chatter marks on the workpiece surface. Finally, the groove is prepared for further cutting tests with the help of a planning process and the process data is stored for the test evaluation.

## 5 RESULTS

For the analysis of the experiments, an evaluation programme is implemented in the MATLAB environment. By loading the stored process data of a cutting test into the evaluation programme, the trajectories and the bisection points are reconstructed. The calculation of new indicator values and the evaluation of the stability criteria is carried out in a cycle time of 0.1 seconds in accordance with [Brecher 2021]. This cycle time enables the algorithm to be applied for in-process chatter detection with low latency. As a comparison, an online frequency domain chatter detection which calculates an FFT every 0.1 s only results in a frequency resolution of 10 Hz which normally is not precise enough for robust detection. In order to quantify the effect of the factors presented in Figure 7 on the chatter detection algorithm, the lower limit value of each stability criteria (see Figure 2) for both indicators (BI and GI) is set as the key value (see Figure 8).

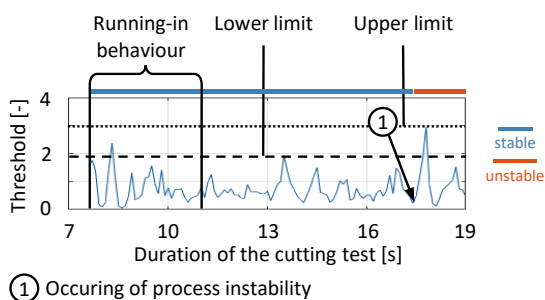


Figure 8 : Procedure for evaluating the cutting tests

The lower limit value of a criterion is defined by the maximum threshold value under stable process conditions and characterises the ideal threshold value for early detection of process instability of a specific cutting test. Since the lower limit value is an empirical value, the limit values of all tests are determined manually, then assigned to the factor stages of an experimental design, averaged and plotted in a diagram. To manually determine the lower limit values, the onset of process stability is first determined using the recorded measurement data. To retrospectively identify the onset of process instability in time domain, the trajectory is examined until a chaotic trajectory is observed, coupled with a significant increase in acceleration amplitude. The lower limit value is finally determined by the maximum value between the decayed run-in behaviour and the onset of process instability (see Figure 8).

In the following test evaluation, the limit criterion is not considered, as the limit criterion was primarily developed for the protection of the machine components than for the early detection of process instability. Figure 9 shows the experimental evaluation of the partial factorial  $2^{7-3}$  experimental design (1). During the cutting tests, full-slot cuts were milled with the workpiece fixed in a vice. The factor stages  $S_1$  and  $S_2$  of the varied factors can be seen in Figure 7 (PF<sub>1</sub>). The test results show that the machine tool and the type of milling tool used have the greatest influence on the shape of the characteristics of the trajectories during the cutting tests and thus on the threshold values of the chatter detection algorithm for both indicators.

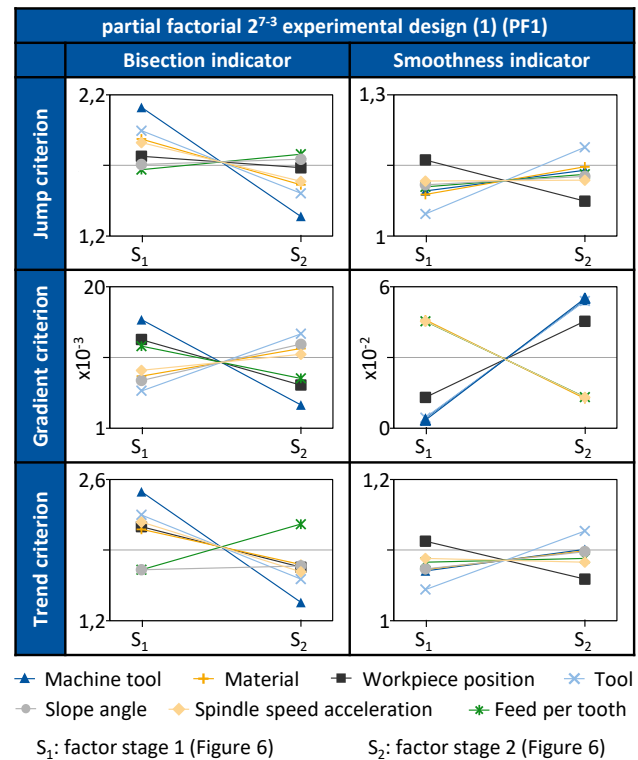


Figure 9 : Evaluation of the partial factorial  $2^{7-3}$  experimental design (1) (PF<sub>1</sub>)

However, it can be seen that the curves for the tool and machine tool of both indicators develop in opposite directions. While the bisection indicator decreases when changing from  $S_1$  to  $S_2$ , the smoothness indicator increases. One possible reason for the different trends is the type of chatter vibrations that occurs. The 5-axis milling machine and the end mill tend to have higher-frequency chatter vibrations compared to the 4-axis milling machine and the milling cutter.

For the given measurement setup, high-frequency chatter vibrations manifest themselves in a less chaotic, more repeatable trajectory (see Figure 4), which means that the deviations of the bisection points are smaller so that the threshold values of the bisection indicator decrease as a result. The relationship between the occurring chatter vibration and the threshold values of the indicators will be discussed again in the course of the evaluation.

The spindle speed acceleration and the slope angle have less influence on the threshold values of the chatter detection algorithm. For the chosen experiments, the effects of the workpiece position as well as the machine tool on the threshold values of the gradient criterion of the smoothness indicator are in a low order of magnitude and are not reflected in the test evaluation of the other two experimental designs. Due to the low number of test repetitions, outliers are more significant. Outliers can be caused by changes in environmental conditions, such as tool wear.

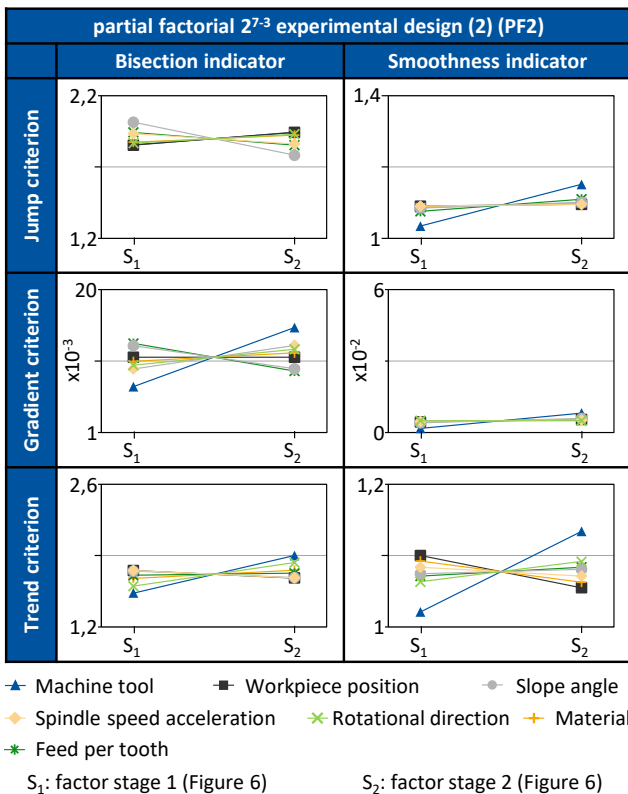


Figure 10 : Evaluation of the partial factorial  $2^{7-3}$  experimental design (2) (PF<sub>2</sub>)

Figure 10 shows the experimental results of the partial factorial  $2^{7-3}$  experimental design (2). In contrast to the partial factorial  $2^{7-3}$  experimental design (1), cuts with an engagement width of 80 % of the tool diameter  $d_w$  are performed instead of a full slot cuts ( $a_e = 100\% \cdot d_w$ ), with the same end mill being used on both machine tools. In addition, the direction of rotation of the milling tool is taken into account. Figure 7 shows the varying factors of the partial factorial  $2^{7-3}$  experimental design (2) (PF<sub>2</sub>), including the factor stages.

From the experimental results, it can be seen that the machine tool has the greatest effect on the threshold values of the chatter detection algorithm, although the effect of the machine tool is less significant compared to the results of the partial factorial  $2^{7-3}$  experimental design (1). At the same time, the machine tool curve of both indicators shows the same trend in the transition from S<sub>1</sub> to S<sub>2</sub> compared to the results of the  $2^{7-3}$  experimental design (1) (see Figure 9). One possible explanation is that during cutting tests with the end mill, high-frequency vibration

components occur during chattering on both the 4-axis and the 5-axis milling machine. This observation is discussed again below. It can also be seen that the influence of the workpiece position, particularly on the threshold values of the gradient criterion of the smooth slope indicator, is lower compared to the partial factorial  $2^{7-3}$  experimental design (1), which supports the assumption of a measurement outlier in the  $2^{7-3}$  experimental design (1). Factors such as the rotational direction or the spindle speed acceleration have a minor effect on the curve characteristics of the trajectories, so that the threshold values of the chatter detection algorithm remain approximately constant.

Finally, the experimental results of the full factorial design are presented in Figure 11. The cutting tests of the full factorial experimental design (2<sup>4</sup>) are carried out exclusively on the 5-axis machine. The clamping system is varied in comparison to the partial factorial  $2^{7-3}$  experimental designs. In addition, the full factorial experimental design is used to verify the observations of the partial factorial  $2^{7-3}$  experimental designs, with regard to the different curves of the measuring position and the influence of the milling tool. The factor stages S<sub>1</sub> and S<sub>2</sub> of the varied factors of the full factorial experimental design can be seen in Figure 7 (FF).

Figure 11 shows that the type of milling tool has the greatest effect on the threshold values of the chatter detection algorithm, as already observed from the results of the partial factorial  $2^{7-3}$  experimental design (1). However, the threshold values of both indicators decrease during the transition from S<sub>1</sub> to S<sub>2</sub>. The observation initially contrasts with the observations from the  $2^{7-3}$  experimental design (1). A possible explanation for the contrast lies in the pronounced compliance behavior of the 5-axis machine over a large frequency range, so that the milling cutter and the end mill contains high-frequency vibration components during chattering. Due to the characteristic of the partial factorial  $2^{7-3}$  experimental designs (1), the pronounced compliance behavior of the 5 axis machine is less significant.

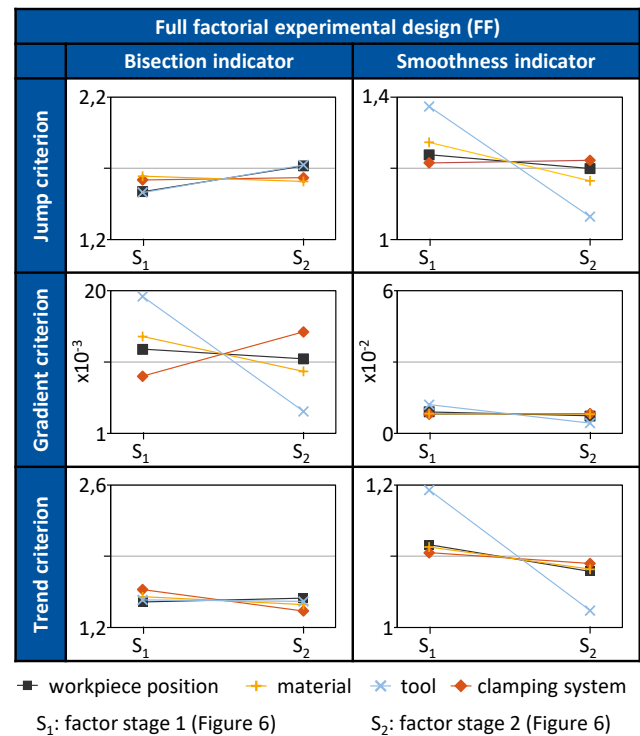


Figure 11 : Evaluation of the full factorial experimental design

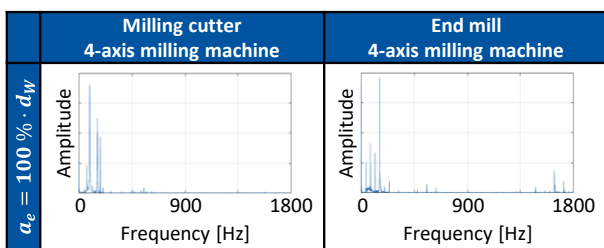
At the same time, the experimental results of the full factorial experimental design confirm the observation of a small effect of the workpiece position on the threshold values of the chatter detection algorithm. A possible explanation for the deviating

observations of the effect of the workpiece position is the limited number of test repetitions, whereby outliers caused by varying test conditions during the cutting tests (e.g. tool wear) are weighted higher.

The type of clamping system and the material have a minor influence on the displacement characteristics of the spindle during a spindle rotation, so that the threshold values of the chatter detection algorithm are almost constant. From the results of all experimental designs, it can be seen that the smoothness indicator is robust to changing boundary conditions compared to the bisection indicator. One possible reason for that is the use of the moving average in the calculation of the smoothness indicator, which acts like a low pass filter, minimising the signal noise of the smoothness indicator. As an interim conclusion, the machine tool used and the milling tool type show the greatest effects on the threshold values of the chatter detection algorithm in the test series.

In order to analyse the effect of the machine tool and the type of milling tool Figure 12 shows the Fast Fourier Transform (FFT) of the acceleration signal during unstable cutting conditions, taking into account the type of milling tool. The FFT is based on cutting tests on the 4-axis milling machine. Figure 12 shows that mainly low frequency chatter vibrations are excited by the milling cutter, especially during cutting tests on the four axis milling machine. During the unstable cutting process, the acceleration spectrum of the end mill also include high frequency vibration components, which can be perceived acoustically.

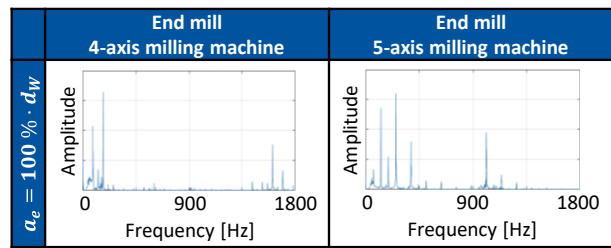
As already mentioned in chapter 2, high-frequency chatter vibrations lead to a slight deviation of the bisection points, resulting in a decrease of the bisection indicator. At the same time, high-frequency vibration components lead to an uneven trajectory, which is well indicated by the smoothness indicator and is accompanied by an increase in the threshold values. Transferring the observations of the acceleration spectrum to the experimental results, a spectral shift of the chatter oscillations and a change in the excited modes requires a change in the threshold values of the chatter detection.



$a_e$  = Engagement width  $d_W$  = Tool diameter

Figure 12 : Frequency spectra of different milling tools using the same milling machine

Figure 13 shows an spectrum of chatter oscillations from the 4-axis and the 5-axis milling machine, using the same end mill. The engagement width during the cutting tests is 80 % of the tool diameter. The spectra show high-frequency vibration components during chattering for both the 4-axis and the 5-axis milling machine. At the same time, the results of the 2<sup>7-3</sup> experimental design (2) shows that the influence of the machine tool on the threshold values of the chatter detection algorithm is less significant when using the same milling tool. This confirms the observation that the characteristics of the occurring chatter oscillation suggest a change in the threshold values of the chatter detection algorithm.



$a_e$  = Engagement width  $d_W$  = Tool diameter

Figure 13 : Frequency spectra of different milling machines using the same milling tool

In addition to the parameter sets, Figure 14 shows the distribution of the cutting tests taken into account for their determination as well as the corresponding success rates. The milling cutter tends to stimulate low frequency structural modes, whereas the end mill stimulates high-frequency spindle-tool modes. To parameterise the chatter detection algorithm, a logic is implemented in the MATLAB development environment that determines optimal threshold values from a number of cutting tests based on the two stability conditions. An exception is the threshold value of the limit criteria, which is determined by the largest lower threshold value of all considered tests.

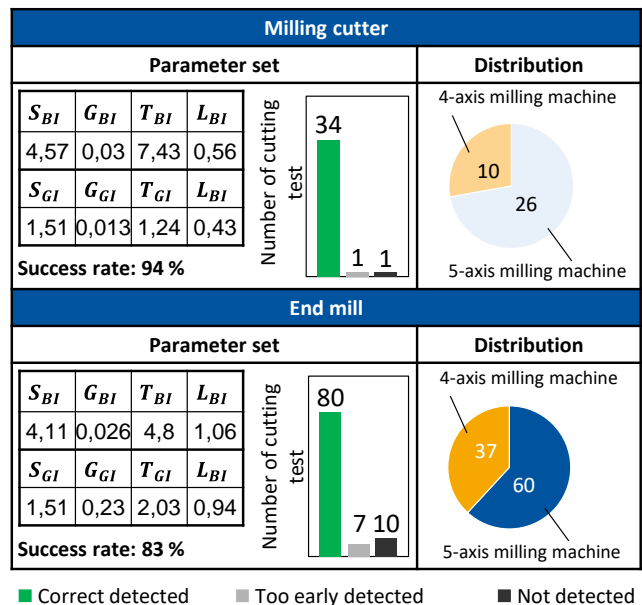


Figure 14 : Parameterisation of the chatter detection algorithm for different milling tools

From the parameterisation of the chatter detection algorithm for the milling cutter it can be noticed that the process instability is correctly indicated in 94 % of the cases. In the subsequent validation, the parameter set has a success rate of 90 %, with a total of 20 cutting tests with the milling cutter considering both stable and unstable cutting tests. The parameter set of the end mill has a lower success rate of 83 % compared to that of the milling cutter.

The success rate of the end mill differs considerably between the two machine tools used in the test series. The success rate of the parameter set for cutting tests on the four-axis milling machine with the end mill is 97 %, whereas the success rate on the five-axis machine is 76 %. The two machine tools used are designed for very different application scenarios. Therefore, the design of the machine structure varies considerably and thus also their dynamical behaviour, which is reflected in the test results and in the success rates.

## 6 CONCLUSION

In this paper the influence of different boundary conditions on the threshold values of a time domain based chatter detection algorithm is analysed. The chatter detection algorithm is the basis for the efficient determination of experimental SLD. [Brecher 2021] In order to strengthen the robustness of the chatter detection algorithm against high-frequency chatter oscillations, an additional indicator, the smoothness indicator, is introduced and integrated into the existing chatter detection algorithm. Subsequently, experimental designs are developed using methods of DoE to systematically investigate the effects of a selection of factors on the chatter detection algorithm. The results of the cutting tests show that a spectral shift of the chatter vibrations or a change in the corresponding mode makes an adjustment in the algorithm's threshold values beneficial. In the final parameterisation of the chatter detection algorithm, the categorisation into parameter sets for the detection of low frequency structural vibrations and high-frequency spindle-tool vibrations shows good success rates. In subsequent investigations, adjustment parameters of the chatter detection algorithm, such as the sampling rate or the number of indicators used for calculating the stability criteria, can be addressed. In addition, the use of a spindle-integrated sensor system offers the potential to reliably detect vibrations with small amplitudes, e.g. chatter vibrations on the workpiece side, due to better transfer behaviour compared to the spindle housing position.

## ACKNOWLEDGMENTS

Funded by the Deutsche Forschungsgemeinschaft (DFG, German Research Foundation) under Germany's Excellence Strategy – EXC-2023 Internet of Production – 39062.

## REFERENCE

- [Altintas 1995] Altintas, Y. and Budak, E. Analytical Prediction of Stability Lobes in Milling. *CIRP Annals*, 1995, Vol. 44, No. 1, pp. 357–362. ISSN 00078506.
- [Altintas 2004] Altintas, Y. and Weck, M. Chatter Stability of Metal Cutting and Grinding. *CIRP Annals*, 2004, Vol. 53, No. 2, pp. 619–642. ISSN 00078506.
- [Altintas 2008] Altintas, Y. et al. Identification of dynamic cutting force coefficients and chatter stability with process damping. *CIRP Annals*, 2008, Vol. 57, No. 1, pp. 371–374. ISSN 00078506.
- [Altintas 2020] Altintas, Y. et al. Chatter Stability of Machining Operations. *Journal of Manufacturing Science and Engineering*, 2020, Vol. 142, No. 11. ISSN 1087-1357.
- [Brecher 2015] Realisierung effizienter Zerspanprozesse: Ergebnisbericht des BMBF Verbundprojekts Reffiz. Aachen: Shaker Verl., 2015. ISBN 978-3-8440-3917-7.
- [Brecher 2017] Brecher, C. et al. Effiziente Ermittlung von Stabilitätsgrenzen: Identifikation von Stabilitätsgrenzen beim Fräsprozess mit variierender Drehzahl. *wt Werkstattstechnik Online*, 2017, Vol. 2017, pp. 313–317.
- [Brecher 2018] Brecher, C. et al. Efficient determination of stability lobe diagrams by in-process varying of spindle speed and cutting depth. *Advances in Manufacturing*, 2018, Vol. 6, No. 3, pp. 272–279. ISSN 2095-3127.
- [Brecher 2021] Brecher, C. et al. Efficient Determination of Stability Lobe Diagrams Deploying an Automated, Data-Based Online NC Program Adaption. *MM Science Journal*, 2021, Vol. 2021, No. 4, pp. 4830–4835. ISSN 18031269.
- [Davies 1998] Davies, M. et al. On the Dynamics of High-Speed Milling with Long, Slender Endmills. *CIRP Annals*, 1998, Vol. 47, No. 1, pp. 55–60. ISSN 00078506.
- [Grossi 2015] Grossi, N. et al. Spindle speed ramp-up test: A novel experimental approach for chatter stability detection. *International Journal of Machine Tools and Manufacture*, 2015, Vol. 89, pp. 221–230. ISSN 08906955.
- [Honeycutt 2016] Honeycutt, A. and Schmitz, T. A New Metric for Automated Stability Identification in Time Domain Milling Simulation. *Journal of Manufacturing Science and Engineering*, 2016, Vol. 138, No. 7. ISSN 1087-1357.
- [Kayhan 2009] Kayhan, M. and Budak, E. An experimental investigation of chatter effects on tool life. *Proceedings of the Institution of Mechanical Engineers, Part B: Journal of Engineering Manufacture*, 2009, Vol. 223, No. 11, pp. 1455–1463. ISSN 0954-4054.
- [Kleppmann 2020] *Versuchsplanung: Produkte und Prozesse optimieren*. München: Hanser, 2020. ISBN 978-3-446-46397-4.
- [Merritt 1965] Merritt, H.E. Theory of Self-Excited Machine-Tool Chatter: Contribution to Machine-Tool Chatter Research—1. *Journal of Engineering for Industry*, 1965, Vol. 87, No. 4, pp. 447–454. ISSN 0022-0817.
- [Navarro-Devia 2023] Navarro-Devia, J.H. et al. Chatter detection in milling processes—a review on signal processing and condition classification. *The International Journal of Advanced Manufacturing Technology*, 2023, Vol. 125, 9-10, pp. 3943–3980. ISSN 0268-3768.
- [Perrelli 2022] Perrelli, M. et al. In-Process Chatter Detection Using Signal Analysis in Frequency and Time-Frequency Domain. *Machines*, 2022, Vol. 10, No. 1, p. 24.
- [Quintana 2008] Quintana, G. et al., A new experimental methodology for identification of stability lobes diagram in milling operations. *International Journal of Machine Tools and Manufacture*, 2008, Vol. 48, No. 15, pp. 1637–1645. ISSN 08906955.
- [Quintana 2011] Quintana, G. and Ciurana, J., Chatter in machining processes: A review. *International Journal of Machine Tools and Manufacture*, 2011, Vol. 51, No. 5, pp. 363–376. ISSN 08906955.
- [Siebertz 2017] Siebertz, K et al., *Statistical experimental design: Design of Experiments (DoE)* (in German). Berlin, Heidelberg: Springer Vieweg, 2017. ISBN 978-3-662-55742-6
- [Yusoff 2011] Yusoff, A. and Sims, N. Optimisation of variable helix tool geometry for regenerative chatter mitigation. *International Journal of Machine Tools and Manufacture*, 2011, Vol. 51, No. 2, pp. 133–141. ISSN 08906955.

**CONTACTS:**

Ralph Klimaschka, M.Sc.

Laboratory for Machine Tools and Production Engineering (WZL) of RWTH Aachen University

Campus-Boulevard 30, 52074 Aachen, Germany

+49 241 80 27930, r.klimaschka@wzl.rwth-aachen.de, <https://www.wzl.rwth-aachen.de>